Transition charge densities at the onset of deformations for even-even $^{98-112}$Ru nuclei

A. J. Singh and P. K. Raina
Department of Physics, H. P. University, Shimla 171005, India
(Received 3 April 1995)

In this paper, we present the Hartree-Fock-Bogoliubov model calculations for transition charge densities of even-even $^{98-112}$Ru nuclei, using the pairing-plus-quadrupole-quadrupole interactions operating in s-d-g-h valence space. It is predicted that the transition charge densities should be able to act as a more sensitive means for clear signature of the shape transitions, which have yet only been looked upon with respect to the changes in the static properties. The static properties calculated from the same model are in good agreement with the available experimental data.

PACS number(s): 21.10.Ft, 21.10.Ky, 21.60.Jz, 25.30.Dh

I. INTRODUCTION

Inelastic electron scattering has played an important role in the electromagnetic probing of the microscopic systems like atoms, molecules, nuclei, and nucleons. The main reason [1–3] that distinguishes it from photonic studies is the advantage of probing the system at continuous values of momentum transfers. Experimental techniques have also gone to the extent that now it is possible to separate the inelastic electron scattering cross sections arising from different excited states for the momentum transfer of 3 fm^{-1} or more in the case of the nuclei. The advantage [2–4] of electromagnetic probing over other types of interaction probes of nuclei is that the strength of interaction is weaker as compared to other types of interactions between the nucleons. The theory describing the scattering process, i.e., quantum electrodynamics is the best understood of all the field theories.

The development of the Fourier-Bessel expansion technique [3–5] employed for transforming the inelastic electron scattering cross-section data into the transition charge densities has opened a very interesting way for the comparison of experiments with theory. Only after the availability of inelastic electron scattering cross-section data for $0^+ \rightarrow 4^+$ excitations in the case of some f-p shell nuclei, has it been possible to observe [6] that the rotor model formula applied to the transformation of static quadrupole moments $Q(2^+)$ and the transition probabilities $B(E2)$ should not be extended as such to a higher multipole. Recently, with the availability of experimental data on transition charge densities for quadrupole and hexadecapole excitations in the case of Pd and Cd nuclei, it has been possible [7,8] to discriminate between the contribution of proton-proton (p-p), neutron-neutron (n-n), and neutron-proton (n-p) parts of two-body effective interactions.

Medium mass nuclei have been the center of activities for quite some time. This is because of the richness in their properties displaying many interesting phenomenon. One interesting observation [9] was in the case of ^{70}Ge, where some anomolous behavior is seen in the transition charge densities experimentally. This has also shown up the potential of inelastic electron scattering in a unique way.

The mass region 100 also provides [10–15] us a nice example of shape transitions. At one end, the nuclei can be described in terms of shell model wave functions involving a small number of configurations and, at the other end, we find good evidences of rotational collectivity. The systematic study of behavior of the low lying collective state of neutron rich even-even Cd, Pd, Ru, and Mo isotopes is of great importance for understanding the gradual change from spherical to a deformed state via transitional phase. These nuclei lie between strongly deformed ^{100}Zr and doubly magic ^{132}Sn near which structural changes are rather rapid with changes in the proton and neutron numbers. These changes have been proposed to be related with exceptionally strong neutron-proton (n-p) interaction [16].

The purpose of this paper is to report the behavior of transition charge densities at the shape transition region in the case of Ru nuclei. Because there is a shape transition taking place in going from ^{98}Ru to ^{112}Ru nucleus, the Ru nuclei with $98<A<102$ seem to be soft vibrators and those with $A>104$ are quasirotors. The ^{104}Ru nucleus is thought to be a transitional nucleus forming zone between soft vibrators on one side and nearly deformed rotors on the other side. This is confirmed by trends of the available experimental data (see Table I) on energy spectra and transition probabilities $B(E2)$. We can notice that for Ru nuclei there is an overall decrease in $E(2_1^+)$ excitation energy in going from ^{98}Ru to ^{112}Ru and also a parallel increase in the ratio $E(4_1^+)/E(2_1^+)$ as well as $B(E2)$ values. This implies that there is an increase in deformation in going from ^{98}Ru nucleus to ^{112}Ru nucleus.

In the past, there have been many attempts to explore the factors responsible for the onset of large deformation in $^{100-106}$Zr and $^{100-106}$Mo nuclei. It is suggested that the neutron-proton (n-p) effective interactions have a deformation producing tendency, while the neutron-neutron (n-n) and the proton-proton (p-p) interactions are of spheriphying nature [11,17]. These ideas have played a crucial role in the development of stretched scheme [18] of Danos and Gillet, rotor model [19] of Arima and Gillet, and the interacting boson model [20] (IBM) of Arima *et al.* In this regard, the role of neutron-proton (n-p) interaction in the spin orbit partner (SOP) in context to the general development of collective features was suggested by Federman and Pittel [11–14,17] and Caston *et al.* [21]. Their calculations provided evidence suggesting that the neutron-proton (n-p) interac-

TABLE I. Some systematics of collective low spin level of even-even Ru nuclei. The $B(E2)$ values are in the units of 10^{-48} e^2 cm^4.

A	$E(2_1^+)$	$E(4_1^+)/E(2_1^+)$	$B(E2)$
98	0.652[a]	2.14	0.392(12)[b]
100	0.539[a]	2.27	0.501(15)[b]
102	0.475[a]	2.33	0.651(16)[b]
104	0.358[a]	2.48	0.841(20)[b]
106	0.270[a]	2.65	
108	0.242[a]	2.75	1.03(14)[b]
110	0.241[a]	2.75	1.11(13)[b]
112	0.237[a]	2.72	1.12(20)[b]

[a]K. Summerer, N. Kaffrell, H. Otto, P. Peuser, and N. Trautman, Z. Phys. A **287**, 287 (1978); K. Summerer, N. Kaffrell, E. Stender, N. Trautman, K. Broden, G. Skarnemark, T. Bjornstad, I. Haldorsen, and J. A. Maruhn, Nucl. Phys. **A339**, 74 (1980); P. de Gellder, D. de Frenne, and E. Jacob, Nucl. Data Sheet **35**, 446 (1982); J. Aysto *et al.*, Nucl. Phys. **A515**, 365 (1990).

[b]S. Raman, C. H. Malarkey, W. T. Miilner, C. W. Nester, Jr., and P. H. Stelson, At. Data Nucl. Data Tables **36**, 21 (1987).

tion between valence nucleons in SOP orbits—the orbits $(g_{9/2})$ and $(g_{7/2})$ in the Zr and Mo nuclei—may be instrumental, viz. the observed onset of large deformation in Mo isotopes with $A>100$. Besides this, it has recently been shown by Khosa, Tripathi, and Sharma [22] that sudden polarizability of the $(g_{9/2})$ shell is responsible for initiating large deformation in neutron rich Mo isotopes.

In this paper, we carry out microscopic study of the yrast band, static quadrupole moment $Q(2^+)$, transition probabilities $BE(2)$, and the transition charge densities for the $^{98-112}$Ru nuclei. Calculations have been done by employing the variation-after-projection (VAP) [23] in conjuction with the Hartree-Fock-Bogolubov (HFB) ansatz for axially symmetric intrinsic wave functions. Whereas the HFB form of wave function permits a consistent treatment of the pairing and deformation degrees of freedom on same footing, the VAP procedure helps in selecting an appropriate intrinsic state for each J through a minimization of expectation value of the Hamiltonian with respect to the states of good angular momenta. The VAP method thus incorporates in the microscopic description the possibility of associating different intrinsic quadrupole deformations with various members of yrast cascade. The full variation after projection framework is preferable to the cranked Hartree-Fock Bogoliubov (CHFB) in which the treatment of angular momentum is only constrained to its correct value on the average. It provides a reasonably satisfactory description of the energies and electromagnetic properties of yrast levels for the quasivibrators as well as quasirotors.

In Sec. II, we present the calculational framework. Section III contains the comparison of the calculated yrast spectra, $Q(2^+)$, as well as $B(E2)$ transition strengths with available experimental results. The theoretical results for transition charge densities and the calculated subshell occupation numbers associated with the ground states of the Ru isotopes are also presented. The last section contains some concluding remarks.

II. CALCULATIONAL FRAMEWORK

A. Projection of states of good angular momentum from the HFB intrinsic states

Here, we briefly discuss the formalism used in our calculations. Pairing correlation between only the like particles has been allowed in our calculations. Employing the usual notations, the axially symmetric intrinsic deformed HFB state with $K=0$ can be written

$$|\phi_0\rangle=\sum_{im}\ (U_i^m+V_i^m b_{im}^\dagger b_{im}^\dagger|0\rangle, \tag{1}$$

where

$$b_{im}^\dagger=\sum_j\ C_{ji}^m a_{jm}^\dagger,$$

$$b_{im}^\dagger=\sum_j\ (-1)^{j-m}C_{ji}^m a_{j-m}. \tag{2}$$

Here, the index i is used to distinguish between different states with same m, and j labels the spherical single particle orbitals. The wave function in Eq. (1) can be reduced to the form

$$|\phi_0\rangle=N\ \exp\left[(1/2)\sum_{\alpha\beta}\ f_{\alpha\beta}a_\alpha^\dagger a_\beta^\dagger\right]|0\rangle, \tag{3}$$

with

$$f_{\alpha\beta}=\sum_i\ C_{j_\alpha i}^{m_\alpha}C_{j_\beta i}^{m_\beta}(V_i^{m_\alpha}/U_i^{m_\beta})m_\alpha^\dagger,-m_\beta^\dagger, \tag{4}$$

where α denotes the quantum numbers (j_α,m_α) and N is the normalization constant.

The state with angular momentum J projected from the HFB state $|\phi_K\rangle$ is given by

$$|\psi_{K=0}^J\rangle=N\int\ d\Omega\ d_{00}^J\ \exp\left(\sum_{\alpha\beta}\ F_{\alpha\beta}(\theta)a_\alpha^\dagger a_\beta^\dagger\right)|0\rangle, \tag{5}$$

where

$$F_{\alpha\beta}(\theta)=\sum_{m'_\alpha}\ \sum_{m'_\beta}\ d^{J_\alpha}_{m_\alpha m'_\alpha}(\theta)d^{J_\beta}_{m_\beta m'_\beta}(\theta)f_{j_\alpha m'_\alpha,j_\beta m'_\beta}. \tag{6}$$

The expression for overlap $\langle\psi_0^J|\psi_0^J\rangle$ is given by (apart from the normalization N)

$$n(\theta)=\langle\psi_0^J|\psi_0^J\rangle=[\det(1+M(\theta)]^{1/2}, \tag{7}$$

where

$$M(\theta)=F(\theta)f^\dagger. \tag{8}$$

The energy of a state with angular momenta J can be written as

$$E_J=\left[\int_0^{\pi} d\theta \sin\theta\, d^J_{00}(\phi)h(\theta)\right] \Big/ \left[\int_0^{\pi} d\theta \sin\theta\, d^J_{00}(\theta)n(\theta)\right]. \tag{9}$$

The intensities of the various angular momenta contained in the intrinsic wave function are given by

$$a_J^2=(1/2)(2J+1)\int_0^{\pi} n(\theta)d^J_{00}(\theta)\sin\theta\, d\theta, \tag{10}$$

the overlap integral $h(\theta)$ is given by

$$h(\theta)=n(\theta)\left[\sum_{\alpha} e_\alpha[M/(1+M)]_{\alpha\alpha}+(1/4)\sum_{\alpha\beta\gamma\delta}\langle\alpha\beta|V_A|\gamma\delta\rangle\left\{2[M/(1+M)]_{\gamma\alpha}[M/(1+M)]_{\delta\beta}\right.\right.$$
$$\left.\left.+\sum_{\nu\rho}[M/(1+M)]_{\gamma\rho}F_{\rho\delta}[1/(1+M)]_{\nu\alpha}f^*_{\nu\beta}\right\}\right] \tag{11}$$

and the overlap integral $n(\theta)$ and $M(\theta)$ are given by Eqs. (7) and (8).

B. Variation after angular momentum projection (VAP) prescription

The VAP procedure involves the selection of an appropriate intrinsic state for each yrast level through a minimization of the expectation value of the Hamiltonian with respect to the states of good angular momentum. We first generate self-consistent HFB solutions, $\phi(\beta)$, by carrying out HFB calculations with the Hamiltonian $(H-\beta Q_0^2)$. The optimum intrinsic state for each yrast lavel, $\phi_{\rm opt}(\beta_J)$, is then selected by ensuring that the following condition is satisfied:

$$\delta[\langle\phi(\beta)|HP^J_{00}|\phi(\beta)\rangle/\langle\phi(\beta)|P^J_{00}|\phi(\beta)\rangle]=0.$$

C. Transition charge density, transition probability, and static electric quadrupole moment for the yrast states

The transition charge density $\rho_L(r)$ is the reduced matrix elements of ρ^{op}_L between the initial and the final nuclear state of spin J_i and J_f and is given by

$$\rho_L(r)=\langle\psi^J_K(\beta')\|\rho^{op}_L\|\psi^J_K(\beta)\rangle. \tag{12}$$

Making use of the general expression [24] for the matrix elements of the irreducible tensor and Eq. (5) for the projected HFB wave functions, we obtained the following expression for the transition charge density:

$$\rho_L(J_i\to J_f)=[n^{J_i}(\beta')n^{J_i}(\beta)]^{-1/2}(2J_i+1)^{-1/2}\int_0^{\pi/2}\sum_{\mu}\begin{vmatrix} J_i & L & J_f \\ -\mu & \mu & 0\end{vmatrix} d^J_{-\mu,0}(\theta)\,\eta(\beta,\beta',\theta)$$
$$\times\left\{\sum_{k,\alpha,\beta} e_k R_{n_\beta l_\beta}(r)R_{n_\alpha l_\alpha}(r)\langle\alpha|Y^L_M|\beta\rangle M(\beta',\beta,\theta)[1+M(\beta',\beta,\theta)]^{-1}\right\}\sin\theta\, d\theta, \tag{13}$$

where $R_{nl}(r)$ is the radial part of the harmonic oscillator state $|nl\rangle$ and the normalizations are given by

$$n^J(\beta)=\int_0^{\pi/2}\eta(\beta,\beta',\theta)d^J_{00}(\theta)\sin\theta\, d\theta, \tag{14}$$

$$\eta(\beta,\beta',\theta)=\{\det[1+M(\beta,\beta',\theta)]\}^{1/2}. \tag{15}$$

The expression for the reduced transition probability for electric 2^2 pole, $B(E2,0^+\to 2^+)$, is given by

$$B(E2,0^+\to 2^+)=(1/16\pi)|\langle\psi^J_K(\beta)\|Q^2_0\|\psi^J_K(\beta)\rangle|^2 \tag{16}$$

and the static quadrupole moment is given by

$$Q(2^+)=\langle\psi^J_K(\beta)\|Q^2_0\|\psi^J_K(\beta)\rangle, \tag{17}$$

where

$$Q^2_\mu=(16\pi/5)^{1/2}r^2Y^2_\mu(\Omega).$$

The expression for the reduced matrix elements of the transition probability can be written as

$$\langle \psi_K^J(\beta)|Q_0^2|\psi_K^J(\beta)\rangle = [n^{J_i}(\beta)n^{J_f}(\beta)]^{-1/2}\int_0^{\pi/2}\sum_{\mu}\begin{vmatrix} J_i & 2 & J_f \\ -\mu & \mu & 0\end{vmatrix} d^J_{-\mu 0}(\theta)\,\eta(\beta,\beta',\theta)\Big\{\sum_{k,\alpha,\beta} e_k\langle n_\alpha l_\alpha|r^2|n_\beta l_\beta\rangle$$

$$\times\langle\alpha|Y^2_M|\beta\rangle\rho^k_{\alpha\beta}(\beta,\beta,\theta)\Big\}\sin\theta\, d\theta, \tag{18}$$

where the density matrix is given by

$$\rho(\theta)=M(\beta,\beta',\theta)/[1+M(\beta,\beta',\theta)]. \tag{19}$$

The initial guess for the wave functions involved in HFB iterations was generated by diagonalizing the Nilsson Hamiltonian and the wave functions $|\phi\rangle$ are obtained by carrying out the HFB calculations. The results of HFB calculations are summarized in terms of the expansion coefficients C^m_{ji} and the amplitudes (V^m_i, U^m_i) appearing in Eq. (1).

These values were used to first calculate $f_{\alpha\beta}$ defined by Eq. (4). We next calculate the matrices F, $[1+M(\theta)]$, and $[1+M(\theta)]^{-1}$ appearing in Eqs. (6), (7), and (8), respectively. Finally we compute the matrix element for transition charge densities, transition probabilities, and static quadrupole moments in Eqs. (13) and (18).

III. RESULTS AND DISCUSSIONS

Transition charge densities and some other properties for even-even $^{98-112}$Ru nuclei

Here in this section, apart from comparing the theoretical results of static properties like energy spectrum, transition probabilities, and static quadrupole moments resulting from VAP prescription in the HFB framework with the available experimental data, we also present some theoretical observations of transition charge densities at the shape transition region in case of $^{98-112}$Ru nuclei.

In the calculations presented here, we have employed the valence space spanned by the $2p_{1/2}$, $1g_{9/2}$, $2d_{5/2}$, $3s_{1/2}$, $2d_{3/2}$, $1g_{7/2}$, and $1h_{11/2}$ shell-model orbits. The single-particle energies (SPE's) corresponding to these shell-model orbits are taken (in MeV) as $\epsilon(2p_{1/2})=-0.8$, $\epsilon(1g_{9/2})=0.0$, $\epsilon(2d_{5/2})=5.4$, $\epsilon(3s_{1/2})=6.4$, $\epsilon(2d_{3/2})=7.9$, $\epsilon(1g_{7/2})=8.4$, and $\epsilon(1h_{11/2})=8.8$. The same set of SPE's have been employed in a number of successful variational model calculations for static and dynamic properties in the mass 100 region by Khosa, Tripathi, and Sharma [22,28] and Singh, Raina, and Dhiman [7,8]. Shell model calculations by Vergados and Kuo [25] in mass region 90 also use the same SPE's after taking $1f_{7/2}$ and $1f_{5/2}$ in the core and lowering down the energy of $1h_{11/2}$ orbit by 1.6 MeV.

The two-body effective interaction that we have employed is of ''quadrupole-quadrupole-plus-pairing'' type. The pairing part of the two body interaction can be written as

$$V_p=-(G/4)\sum_{\alpha\beta} S_\beta S_\alpha a^\dagger_\alpha a^\dagger_{\bar\alpha} a_\beta a_{\bar\beta},$$

where α denotes the quantum numbers $(nljm)$. The state $\bar{\alpha}$ is the same as α but with the sign of m reversed. Here S is the phase factor $(-1)^{j-k}$. The q-q part of the two-body interaction is given by

$$V_{q\text{-}q}=-(X/2)\sum_{\alpha\beta\gamma\delta}\sum_{\mu}\langle\alpha|q^2_\mu|\gamma\rangle\langle\beta|q^2_{-\mu}|\delta\rangle \times(-1)^\mu a^\dagger_\alpha a^\dagger_\beta a_\delta a_\gamma,$$

where the operator q^2_μ is given by

$$q^2_\mu=(16\pi/5)^{1/2}r^2Y^2_\mu(\theta,\phi).$$

The strengths for the like particle neutron-neutron (n-n) and proton-proton (p-p) components of the q-q interaction are taken as $X_{\pi\pi}=X_{\nu\nu}=-0.0105$ MeV b^{-4} and the n-p component is taken as $X_{\pi\nu}=-0.0231$ MeV b^{-4}. Here b is the oscillator parameter. These values for the strengths of the q-q interactions are comparable to those suggested by Arima [26] on the basis of an empirical analysis of the effective interactions. The strength of the pairing interaction was fixed (through the approximate relation $G=18/A$) at $G=0.18$ MeV.

1. Yrast spectra

In Fig. 1, we have presented observed experimental as well theoretical yrast spectra for $^{98-112}$Ru nuclei resulting from VAP prescription. From Fig. 1, one can observe that the theoretical results are in good agreement with the experimental ones.

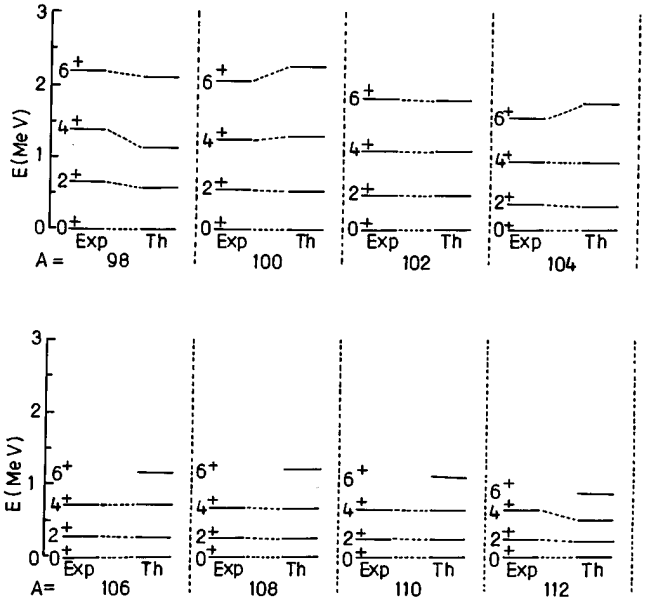

FIG. 1. Experimental spectra of low lying states of the even-even $^{98-112}$Ru isotopes along with theoretical results in VAP on HFB states.

TABLE II. The intrinsic quadrupole moments of the HFB states in some doubly Ru isotopes. Here $\langle Q_0^2\rangle_\pi$ ($\langle Q_0^2\rangle_\nu$) gives the contribution of the protons (neutrons) to the total intrinsic quadrupole moment. The quadrupole moments have been computed in units of $b=1.01A^{1/6}$ fm.

A	$E_{\rm HFB}$	$\langle Q_0^2\rangle_{\rm HFB}$	$\langle Q_0^2\rangle_\pi$	$\langle Q_0^2\rangle_\nu$
98	11.91	30.06	13.17	16.89
100	22.57	36.76	14.89	21.87
102	35.22	37.91	15.24	22.67
104	45.69	66.19	24.29	41.90
106	59.06	70.49	25.97	44.52
108	73.77	73.82	27.28	46.54
110	88.31	72.06	26.66	45.40
112	104.25	68.43	25.30	43.13

2. Transition probabilities and static quadrupole moments

We now move on to the discussion of electromagnetic properties of yrast levels in $^{98-112}$Ru nuclei. In Table II, we have given the HFB results for the total HFB energy $E_{\rm HFB}$ and total quadrupole moment ($\langle Q_0^2\rangle_{\rm HFB}$) along with the separate contribution of quadrupole moment for proton ($\langle Q_0^2\rangle_\pi$) as well as that of neutron ($\langle Q_0^2\rangle_\nu$). Here, we notice that the deformation goes on increasing slowly from ^{98}Ru to ^{102}Ru nucleus. But in going from ^{102}Ru to ^{104}Ru there is a sudden change in the deformation with smooth increase up to ^{108}Ru and then decrease as we go to ^{112}Ru. In Table III, we have presented calculated theoretical values of the transition probabilities $B(E2;0^+\rightarrow 2_1^+)$ and static quadrupole moments $Q(2_1^+)$ values along with the experimental values. Present microscopic description permits an adequate interpretation of available electromagnetic data in terms of a reasonable variation of isoscalar effective charge; computed $B(E2)$ and $Q(2_1^+)$ values are consistent with the experiments, for the isoscalar effective charges $e_{\rm eff}=0.8$ for $^{98-100}$Ru, $e_{\rm eff}=0.9$ for ^{102}Ru, $e_{\rm eff}=0.5$ for ^{104,106}Ru, and $e_{\rm eff}=0.6$ in case of ^{110,112}Ru. Observed small increase in the isoscalar effective charge in the present work may arise from the contributions of the polarization of the ^{76}Sr core and are likely to be correlated with the magnitude of the deformation due to valence

TABLE III. Comparison of the calculated and observed $B(E2,0^+\rightarrow 2_1^+)$ and $Q(2_1^+)$ values in some Ru isotopes. The effective charges have been used such that for protons the effective charge is $e=1+e_{\rm eff}$ and for neutrons it is $e=e_{\rm eff}$. The $B(E2;0^+\rightarrow 2_1^+)$ values are in the units of 10^{-48} e^2 cm^4 and the $Q(2_1^+)$ values have been given in the units of 10^{-24} cm^2.

		$B(E2,0^+\rightarrow 2_1^+$		$Q(2_1^+)$	
A	(e_π,e_ν)	Calc.	Expt.	Calc.	Expt.
98	(1.8,0.8)	0.351	0.392(12)[a]	−0.209	−0.20(9)[b]
100	(1.8,0.8)	0.486	0.501(10)[a)]	−0.270	−0.20(7)[b]
102	(1.9,0.9)	0.614	0.651(16)[a]	−0.300	−0.35(7)[b]
104	(1.5,0.5)	0.799	0.841(16)[a]	−0.350	−0.35(8)[b]
106	(1.5,0.5)	0.915		−0.380	
108	(1.5,0.5)	1.04	1.03(14)[a]	−0.456	
110	(1.6,0.6)	1.224	1.11(13)[a]	−0.501	
112	(1.6,0.6)	1.120	1.12(20)[a]	−0.489	

[a]S. Raman, C. H. Malarkey, W. T. Milner, C. W. Nester Jr., and P. H. Stelson, At. Data Nucl. Data Tables **36** 21 (1987).
[b]P. Raghavan, At. Data Nucl. Data Tables **42**, 189 (1989).

TABLE IV. (a) The calculated values of the occupation numbers of various orbits in the ground states of some Ru isotopes for protons. (b) The calculated values of the occupation numbers of various orbits in the ground states of some Ru isotopes for neutrons.

(a)

A	$3s_{1/2}$	$2p_{1/2}$	$2d_{3/2}$	$1d_{5/2}$	$1g_{7/2}$	$1g_{9/2}$	$1h_{11/2}$
98	0.00	1.60	0.00	0.16	0.01	4.15	0.07
100	0.01	1.46	0.00	0.23	0.01	4.17	0.11
102	0.01	1.44	0.00	0.25	0.01	4.19	0.10
104	0.13	0.13	0.09	0.93	0.08	4.71	0.00
106	0.22	0.07	0.21	1.01	0.14	4.39	0.00
108	0.28	0.05	0.31	1.05	0.18	4.19	0.00
110	0.25	0.06	0.26	1.32	0.16	4.32	0.00
112	0.18	0.09	0.16	0.98	0.11	4.55	0.00

(b)

A	$3s_{1/2}$	$2p_{1/2}$	$2d_{3/2}$	$1d_{5/2}$	$g_{7/2}$	$1g_{9/2}$	$1h_{11/2}$
98	0.52	1.99	0.24	3.06	0.09	9.95	0.13
100	0.67	1.99	0.89	3.66	0.57	9.94	0.26
102	0.83	1.99	1.15	4.33	1.03	9.93	0.72
104	0.72	1.99	1.39	2.80	1.89	9.77	3.44
106	0.76	1.99	1.44	3.09	2.49	9.76	4.45
108	0.80	1.99	1.49	3.40	2.94	9.79	5.57
110	1.02	1.99	1.68	3.88	3.56	9.85	6.00
112	1.11	1.99	1.75	4.55	4.22	9.93	6.43

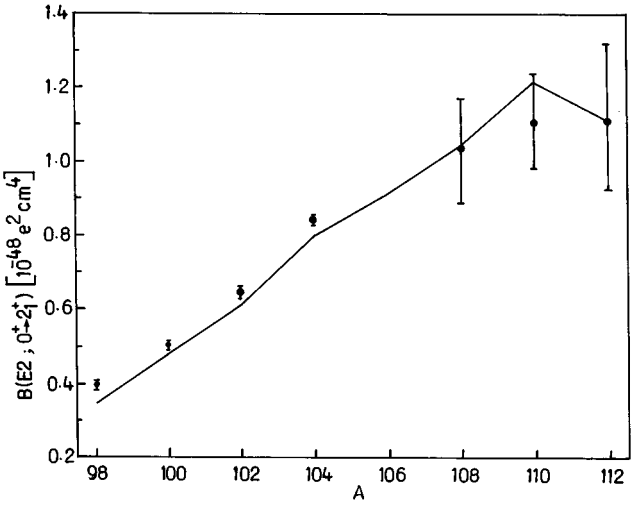

FIG. 2. The $B(E2)$ values for the even-even Ru isotopes. The experimental values are represented by full circles with estimated error bars and the points joined by the solid line represent the theoretical results.

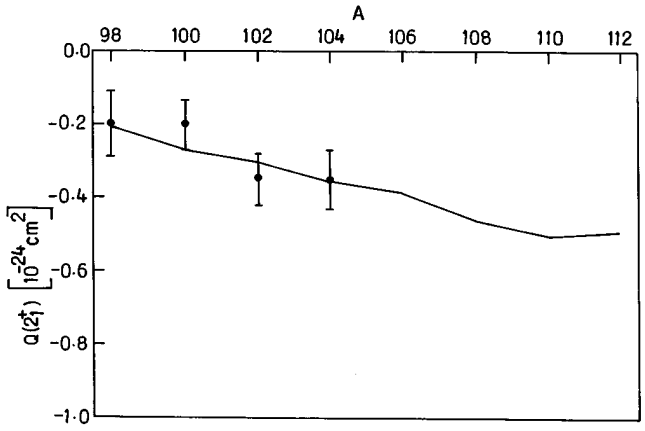

FIG. 3. The $Q(2_1^+)$ values for the even-even Ru isotopes. The experimental values are represented by full circles with estimated error bars and the points joined by the solid line represent the theoretical results.

particles. There is a sudden jump in the $B(E2)$ values (see Fig. 2) in going from ^{102}Ru to ^{104}Ru and continues increasing to ^{110}Ru and then starts decreasing. Static quadrupole moments (see Fig. 3) also show similar behavior. Such theoretical observations [27] were also reported by Isacker and Puddu through IBM calculations of $B(E2)$ and $Q(2_1^+)$ values for these nuclei. The changes in yrast spectra and transition probabilities can be understood in terms of subshell occupancy of protons and neutrons to different shell-model orbits as discussed below.

3. Occupation numbers for shell-model orbits

In Tables IV(a) and IV(b), we have given the results for the occupation numbers of protons and neutrons for the shell-model orbits $2p_{1/2}$, $3s_{1/2}$, $2d_{3/2}$, $2d_{5/2}$, $1g_{7/2}$, $1g_{9/2}$, and $1h_{11/2}$ in the ground states of the nuclei $^{98-112}$Ru. Here one finds that the onset of large deformation in these nuclei is seen to be characterized by significant change in the occupation numbers to different shell-model orbits. From the Fig. 4 it is observed that the occupation numbers for $(1d_{5/2})$ orbits increases and occupation numbers of $(2p_{1/2})$ orbits decreases in going from ^{98}Ru to ^{110}Ru and the occupation number of $d_{5/2}$ then decreases. The occupation numbers for $(1h_{11/2})$, $(1g_{7/2})$, and $(1d_{3/2})$ orbits increases on the addition of neutrons while the occupation numbers for $(1d_{5/2})$ first increases from ^{98}Ru to ^{102}Ru then decreases for ^{104}Ru and again goes on increasing. The large deformation of ^{104}Ru is due to a noticeable decrease in occupation numbers of $(2p_{1/2})$ orbit from the value 1.44 to 0.13 and simultaneous increase in occupation numbers of $(1d_{5/2})$ and $(1g_{9/2})$ orbits from the value 0.25 and 4.19 to 0.93 and 4.71, respectively. The occupation numbers for $(1d_{5/2})$ orbit decreases suddenly from the value 4.33 to 2.89 while that of $(1h_{11/2})$ orbits increases from the value 0.72 to 3.44, respectively. These sudden changes in occupancy of protons as well as neutrons to different orbits for ^{104}Ru are prominently reflected on the electromagnetic properties of yrast levels discussed above.

Similar to the earlier observations [28] made by Sharma, Tripathi, and Khosa for Mo nuclei, our study on Ru nuclei does not reveal any significant simultaneous increase or decrease of $(1g_{9/2})$ and $(1g_{7/2})$ occupancies at $A=100$. Thus our results also do not validate the earlier suggestion concerning the role of n-p interaction between the valence nucleons in SOP. Kratz *et al.* [29] have tried to extract information on pairing reduction and the related onset of the deformation in some neutron-rich odd-odd $A=100$ nuclei by examining the available data on the β-decay half-lives $\log ft$ values, and energies of the two quasiparticle states in the framework of the shell model involving the random phase approximation. These calculations have also demonstrated that n-p interaction of the SOP parentage is of little importance, viz. a total collapse of pairing in these nuclei.

4. Transition charge densities for $0^+ \rightarrow 2^+$ excitations

After going through the static properties for Ru isotopes now we move on to discussion of the transition charge densities for the quadrupole excitation of Ru isotopes. The results for transition charge densities for $0^+ \rightarrow 2_1^+$ excitations are presented in Fig. 5. The effective charge prescription which is used in order to include the renormalizations in a simple way gives only quantitative changes and does not show any qualitative change. Thus the transition charge densities do not seem to obey the effective charge prescriptions. From Fig. 5, we can notice the clear cut changes in the transition charge densities as we go from ^{98}Ru to ^{112}Ru. The magnitude of the surface peak located near 5 fm increases on the addition of the neutrons from $^{98-108}$Ru nuclei and then decreases in going from $^{110-112}$Ru nuclei. Some sharp changes are also noticed in the interior of these nuclei. There is the emergence of one negative peak at 1 fm and the other positive peak at 2.5 fm whose magnitudes increase as we move from ^{98}Ru to ^{108}Ru nuclei and then there is a slow decrease. As noticed for static properties, the transition charge densities also show sudden change in going from ^{102}Ru to ^{104}Ru nucleus. The magnitude of the positive surface peak near 5 fm and negative peak at 1 fm suddenly

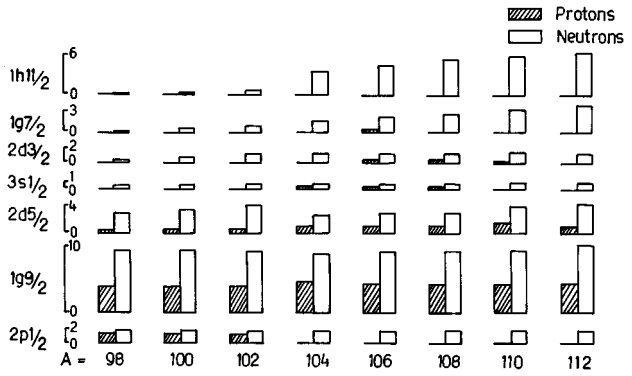

FIG. 4. Theoretical results of subshell occupation numbers in the ground states of the even-even Ru isotopes.

increases from 1.10×10^2 e fm^{-3} and 0.11×10^2 e fm^{-3} to 1.59×10^2 e fm^{-3} and 0.41×10^2 e fm^{-3}, respectively. These changes in transition charge densities can also be correlated with occupancy of subshell orbits as discussed in the case of the static properties, however, here the effects are prominently reflected.

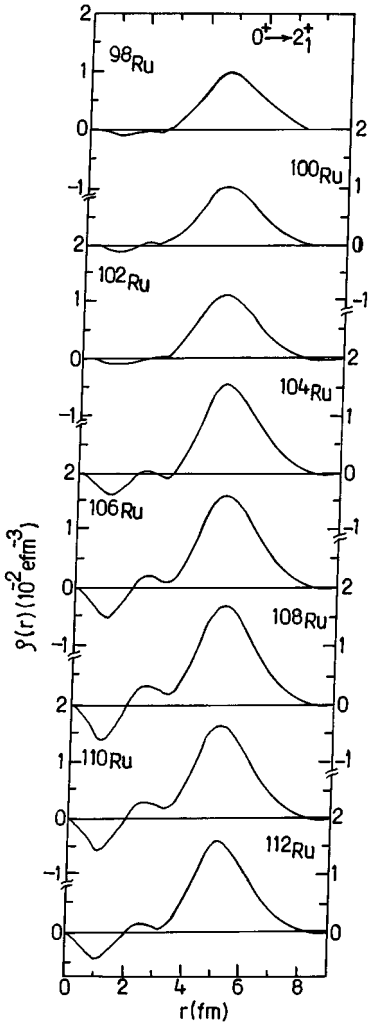

FIG. 5. Transition charge densities for $0^+\rightarrow2_1^+$ excitations for the even-even $^{98-112}$Ru isotopes.

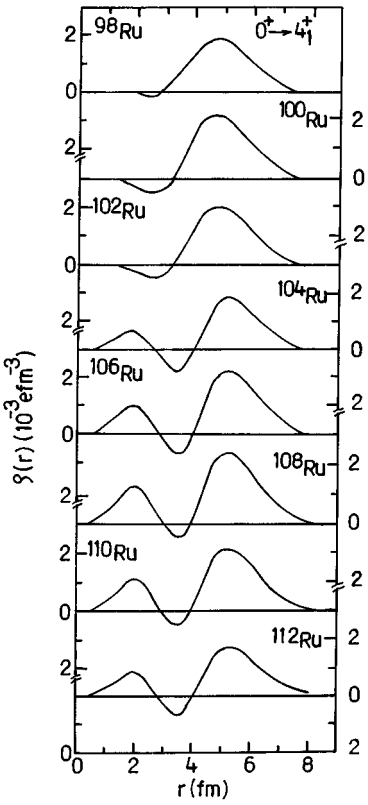

FIG. 6. Transition charge densities for $0^+\rightarrow4_1^+$ excitations for the even-even $^{98-112}$Ru isotopes.

5. Transition charge densities for $0^+\rightarrow4^+$ excitations

We have also given the theoretical results for hexadecapole excitations for Ru nuclei in Fig. 6. Here again we observe a similar trend as in the case of the quadrupole excitations. Apart from the change in overall amplitudes, which is almost five times less in the case of the hexadecapole excitations as compared to the quadrupole excitations, here the changes are more drastic. In the interior, a negative peak appears around 2.5 fm, whose magnitude goes on increasing as we move from ^{98}Ru to ^{108}Ru and then goes on decreasing. The position of this negative peak gets shifted continuously to 3.5 fm on reaching the ^{106}Ru nucleus and then gets fixed. There is a similar shift of 0.5 fm in the surface peak too. The changes in the magnitudes as well as the positions of these peaks and the emergence of a positive peak around 2 fm, while going from ^{102}Ru to ^{104}Ru nucleus, are some distinct features for the hexadecapole excitations of these nuclei.

IV. CONCLUSION

The success in the results of transition charge densities for the quadrupole excitations [7,8] in the case of ^{106,110}Pd and ^{110,114}Cd nuclei with the quadrupole-quadrupole-plus-pairing interactions has led us to believe that the results for quadrupole excitations in the case of Ru nuclei should also be reliable. The observed dramatic onset of the large deformations around $A=100$ can be understood in terms of the polarizations of conventional ($Z=40$, $N=50,56$) cores and the par-

ticipation of the $1h_{11/2}$ orbit in the valence space. Our calculations of transition charge densities in Ru nuclei show quite prominent changes for the quadrupole as well as hexadecapole excitations at the shape transition regions. The systematic experimental data for these nuclei can be very useful for the understanding of the behavior of different excitations clearly and can help in better understanding of the phenomenon in this region.

[1] T. De. Forest and J. D. Walecka, Adv. Phys. **57**, 15 (1966).
[2] H. Uberall, *Electron Scattering From Complex Nuclei, Part A & B* (Academic, New York, 1971).
[3] J. Heisenberg and H. P. Block, Annu. Rev. Nucl. Part. Sci. **33**, 569 (1983).
[4] J. Heisenberg, *Advances in Nuclear Physics, Vol. 12* (Plenum, New York, 1981), p. 66.
[5] B. Frois and C. N. Papanicolas, Annu. Rev. Nucl. Part. Sci. **37**, 133 (1987).
[6] S. K. Sharma and P. K. Raina, Phys. Rev. C **42**, 635 (1990).
[7] A. J. Singh, P. K. Raina, and S. K. Dhiman, Phys. Rev. C **50**, 2307 (1994).
[8] A. J. Singh, Ph.D. thesis, H. P. University, 1993.
[9] J. P. Bazantay *et al.*, Phys. Rev. Lett. **54**, 643 (1985).
[10] E. Cheifetz, R. C. Jared, S. G. Thompson, and J. B. Wilhelmy, Phys. Rev. Lett. **25**, 38 (1970); D. Hook *et al.*, J. Phys. G **12**, 1277 (1986).
[11] P. Federman and S. Pittel, Phys. Lett. **69B**, 385 (1977).
[12] P. Federman and S. Pittel, Phys. Lett. **77B**, 29 (1978).
[13] P. Federman, S. Pittel, and R. Campos, Phys. Lett. **82B**, 9 (1979).
[14] P. Federman and S. Pittel, Phys. Rev. C **20**, 820 (1979).
[15] S. Pittel, Nucl. Phys. **A347**, 417 (1979).
[16] J. Eberth, R. A. Meyer, and K. Sistemich, *Proceedings of the International Workshop on Nuclear Structure in the Zirconium Region*, Bad Honnef, 1988 (Springer, Berlin, 1988).
[17] C. K. Nair, A. Ansari, and L. Satpathy, Phy. Lett. **71B**, 257 (1977).
[18] M. Danos and V. Gillet, Phys. Rev. **61**, 1034 (1967).
[19] Arima and Gillet, Ann. Phys. (N.Y.) **66**, 17 (1971).
[20] A. Arima, T. Otsuka, F. Iachello, and I. Talmi, Phys. Lett. **B6**, 205 (1977).
[21] R. F. Caston *et al.*, Phys. Rev. Lett. **47**, 1433 (1981).
[22] S. K. Khosa, P. N. Tripathi, and S. K. Sharma, Phys. Lett. **119B**, 257 (1982).
[23] L. Satpathy and S. C. K. Nair, Phys. Lett. **26B**, 257 (1968); R. Driezler, P. Federman, B. Giraud, and E. Ormes, Nucl. Phys. **A113**, 145 (1968); J. Vojtik, *ibid*. **A212**, 131 (1973); E. Caurier and B. Grammaticos, *ibid*. **A279**, 333 (1977); S. K. Sharma, *ibid*. **A260**, 226 (1976).
[24] N. Onishi and S. Yoshida, Nucl. Phys. **A80**, 367 (1966).
[25] J. D. Vergodos and T. T. S. Kuo, Phys. Lett. **35B**, 93 (1971).
[26] A. Arima, Nucl. Phys. **A354**, 19 (1981).
[27] P. Van Isacker and G. Puddu, Nucl. Phys. **A348**, 125 (1980).
[28] S. K. Sharma, P. N. Tripathi, and S. K. Khosa, Phys. Rev. C **38**, 2935 (1988).
[29] K. L. Kratz *et al.*, Phys. Lett. **119B**, 17 (1982).